# Time Domain Filter Comparison in Passive Radar Systems

**Tamas Peto, Rudolf Seller**

Broadband Infocommunication and Electromagnetic Theory, Budapest University of Technology and Economics
Egry József str., 18, 1111 Budapest, HUNGARY
email: peto@hvt.bme.hu, seller@hvt.bme.hu

***Abstract:*** *The detection performance of a passive radar systems is generally determined by the received reference and surveillance signals purity. In recent times a number of interference cancellation techniques have been researched to deal with the disturbances on the surveillance channel. The variety of different methods operate in the space, time and frequency domains with having different implementations. This paper aims to examine and compare the performances of the fundamental temporal filtering methods in real environment using field measurement data.*

## 1. Introduction

A very significant limitation factor of the proper operation of passive radars is the so-called masking effect [1]. This undesired effect limits the detection capabilities when the surveillance channel contains unwanted reference correlated signal components in addition to the useful target reflection. In recent times the Zero Doppler Interference Supression (ZDIS) is an actively researched field of the passive radars [3], [5], [6], [7], [8], [9], [10], [11].

The suppression of the undesired interferences are often realized in the space domain via the application of antenna systems and digital beamforming techniques. The operation and effectiveness of fixed and adaptive beamformers are widely inspected in passive radar scenarios in [7].

Beside the application of spatial filtering by means of digital beamforming the adaptive temporal cancellation methods also have significant role in the ZDIS. These techniques in passive radar scenario utilizes the available reference signal to cancel out the zero Doppler shifted and delayed replicas of the transmitted illumination signal. These procedures are quite different in implementation or the subspace selection but solve the Wiener filtering problem without exception. The resulting FIR (Finite Impulse Response) filter produce the sum of the properly weighted and delayed replicas of the reference signal, which is then subtracted from the surveillance channel.

As these algorithms are trying to properly estimate the current impulse response of the environment, stationarity is very important. Cardinali et al. compared the available iterative Wiener filtering techniques in passive radar scenario such as the LMS (Least Mean Square), NLMS (Normalized Least Mean Square), RLS (Recursive Least Mean Square) algorithms [10]. In contrast to the iterative solutions, which adapt the weight coefficients sample by sample the


978-3-7369-9343-3 

ECA (Extensive Cancellation Algorithm) apply the SMI (Sample Matrix Inversion) method to estimate the inverse of the temporal correlation matrix on the whole coherent signal processing batch [11]. As the environment is often not stationary during the CPI (Coherent Processing Interval) the estimation of the filter coefficient can be more accurate using shorter batches. This filter modification is investigated by F. Colone et al. in [3], [6]. Cardinali et al. compared the LMS, NLMS, RLS and also the ECA algorithms in [10] by evaluating the clutter attenuation on simulated scenarios.
The ultimate goal of this paper is to present a relevant and objective performance comparison of the currently available interference cancellation techniques applied in passive radar systems. To achieve this aim, field measurement result are evaluated using the so far researched algorithms. To compare their performances a detected target is analyzed along its trajectory. The performance metric used in this research is the achieved target Signal to Interference and Noise Ratio (SINR).

## 2. Method of algorithm performance evaluation

The performance of the different filtering methods are compared using their achieved improvement in the range-Doppler matrix. The demonstrator hardware used for this experiment is a quad channel passive radar receiver. The detailed description of this hardware can be found in [4]. From among the four receiver channel one is used as the reference channel and the remaining three channel are used as the surveillance channels. To investigate the performance of temporal filtering techniques only the first antenna channel is selected from the surveillance antenna array. The relevant target SINR values are obtained from field measurement data using DVB-T signal as the Illuminator of Opportunity (IoP) at $f = 634MHz$. The measurements were taken near to Ferenc Liszt international airport at Budapest. In the test measurement several landing airplanes have been recorded. The saved offline data is then processed with the different algorithms. At the output of the processing the SINR of the captured airplane have been extracted from the RD matrix. The CPI used for all the measurements described in this paper is $125ms$. The presented algorithm performance improvements are relative to the results obtained when no filtering is applied. More details about the measurement scenario and the configuration can also be found in [7].

## 3. Temporal filtering techniques

Time domain filtering techniques utilize the available reference channel $x_r[n], n = 0 \dots N-1$ to cancel out the time delayed and Doppler shifted replicas of the transmitted illuminator signal. The number of samples in a CPI is denoted by $N$. This filtering concept assumes a linear channel model, thus solves the Wiener filtering problem to obtain the filter coefficient for a trasversal filter. The structure of the adaptive time domain filter is illustrated in figure 1.

The filtered output samples $x_f[n]$ are calculated by the subtracting the time delayed samples of

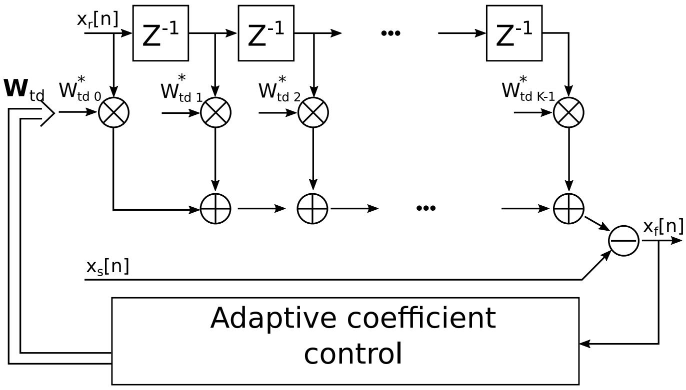


Figure 1: Adaptive time domain filter structure

the reference signal $x_r[n-i], i = 0, 1 \dots$ from the surveillance signal samples $x_s[n]$.

$$x_f[n] = x_s[n] - \boldsymbol{w}_{td}^H \boldsymbol{x_r}[n], \tag{1}$$

where the $\boldsymbol{x_r}[n]$ vector denotes the last $K$ samples of the reference channel and $\boldsymbol{w}_{td}$ is the filter coefficient vector that is calculated adaptively from the input channels $\boldsymbol{w}_{td} \in \mathrm{C}^{K \times 1}$.

$$\boldsymbol{x_r}[n] = \begin{bmatrix} x_r(n) & x_r(n-1) & \dots & x_r(n-K+1) \end{bmatrix}^T \tag{2}$$

The adaptive coefficient control block estimates the surveillance channel parameters with a linear model by minimizing the Mean Squared Error (MSE) at the output of the filter. In case of passive radars, it is the filtered surveillance channel $x_f[n]$.

$$\underset{\boldsymbol{w}_{td}}{min} \mathrm{E}\left\{ |x_f[n]|^2 \right\} \tag{3}$$

Solving 3 results in the well known Wiener-Hopf equation.

$$\boldsymbol{w}_{td} = \boldsymbol{R_t}^{-1} \boldsymbol{r_t}, \tag{4}$$

where $\boldsymbol{R_t}$ is the autocorrelation matrix of the reference signal and $\boldsymbol{r_t}$ is the cross-correlation vector of the time delayed replicas of the reference signal and surveillance signal.

$$\boldsymbol{R_t} = \mathrm{E}\left\{ \boldsymbol{x_r}[n] \boldsymbol{x_r}[n]^H \right\} \tag{5a}$$

$$\boldsymbol{r_t} = \mathrm{E}\left\{ x_s[n]^* \boldsymbol{x_r}[n] \right\} \tag{5b}$$

In real cases the $\boldsymbol{R}_t$ and $\boldsymbol{r}_t$ are not known, thus we have to estimate them from the measured data. The following presented algorithms are all differ in the estimation techniques. The Sample Matrix Inversion (SMI) and the Extensive Cancellation Algorithm (ECA) use the whole CPI for the estimation. In contrast the batches version of the ECA algorithm (ECA-B) use smaller fractions of the CPI. While the iterative LMS, NLMS and RLS algorithms produce new estimation for every new signal sample.

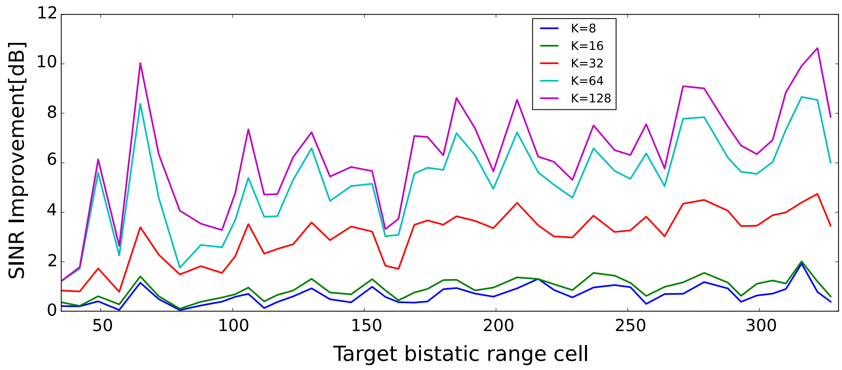


Figure 2: SMI algorithm improvements with different filter dimensions

### 3.1. Sample matrix inversion

The most obvious filter coefficient calculation method is the SMI which use the sample average to estimate the real values. The filter output using the SMI technique in matrix form can be written as follows:

$$\boldsymbol{x}_f = \left(\boldsymbol{I} - \boldsymbol{X}\left(\boldsymbol{X}^H\boldsymbol{X}\right)^{-1}\boldsymbol{X}^H\right)\boldsymbol{x}_s, \tag{6}$$

where $\boldsymbol{x}_f \in \mathrm{C}^{N\times1}$ is the vector of the filtered output signal, $\boldsymbol{x}_s \in \mathrm{C}^{N\times1}$ is the surveillance signal vector, and $\boldsymbol{X} \in \mathrm{C}^{N\times K}$ is the signal subspace matrix, which is composed of the time delayed replicas of the reference signal vector $\boldsymbol{x}_r \in \mathrm{C}^{N\times1}$ and $\boldsymbol{I} \in \mathrm{C}^{N\times N}$ is an identity matrix.

$$\boldsymbol{X} = \begin{bmatrix}\boldsymbol{x_r} & \boldsymbol{D}\boldsymbol{x_r} & \dots & \boldsymbol{D}^{K-1}\boldsymbol{x_r}\end{bmatrix} \tag{7}$$

In 7 $\boldsymbol{D}$ is a permutation matrix, that applies time delay on the rerence signal vector by one sample. The detailed formulalation can be found in [6].
In this calculation method the only configurable parameter is the depth of the filter $K$. Results obtained with the SMI implementation of the time domain filter can be seen in figure 2. The curves in the figure show the achieved improvements for increasing filter dimension. It can be observed that as the target approaches to the radar the gain of the filtering decreases as the same amount of cancelled clutter power does not grant the same target SINR improvements when the $SINR_{target}$ is high enough. As expected the achieved improvement increases for higher $K$ values. However there is no reason to increase $K$ after a certain value, as further improvements are negligible. We must also note that the optimal value of $K$ is environment specific. Range-Doppler matrix calculated with the SMI coefficient calculation method for $K = 128$ can be seen in figure 8a. A deep null can be clearly identified at the zero Doppler line from $0$ to the $128$th range cell.

### 3.2. ECA

The standard transversal filter structure can effectively remove the time delayed replicas of the reference channel which are zero Doppler shifted. In case the environment is not static the clutter also has non zero Doppler shifted components from slowly moving ground objects like trees or vegetation. In order to deal with these effects the ECA algorithm expands the signal subspace $\boldsymbol{X}$ with the Doppler shifted versions of the reference signal and its time delay replicas. The extended reference signal subspace matrix has the following form:

$$\boldsymbol{X}' = \left[\boldsymbol{\Lambda}_{-P}\boldsymbol{X} \quad \boldsymbol{\Lambda}_{-P+1}\boldsymbol{X} \quad \dots \quad \boldsymbol{\Lambda}_{-1}\boldsymbol{X} \quad \boldsymbol{X} \quad \boldsymbol{\Lambda}_{1}\boldsymbol{X} \quad \dots \quad \boldsymbol{\Lambda}_{P-1}\boldsymbol{X} \quad \boldsymbol{\Lambda}_{P}\boldsymbol{X}\right], \tag{8}$$

where $\boldsymbol{\Lambda}_i$ is a matrix which applies Doppler shift on the transformed vector with a frequency equal with $i$ Doppler bin. This method is first described by F. Colone and P. Lombardo in [11] and currently exist a number of different modifications such as ECA-B, ECA-S, ECA-C and ECA-CD [6], [3], [5], [8]. In its basic form it uses the whole CPI to calculate the corresponding filter coefficient. The filtered output signal is calculated using 6 with the replacement of $\boldsymbol{X}$ by $\boldsymbol{X}'$. Configuration of the filter is done with choosing the time domain depth $K$ and Doppler domain depth $P$ parameters. It must be emphasized that care must be taken while specifying the Doppler domain depth as unreasonably high values can result in cancelling the useful target reflection also. Figure 8b shows the RD matrix obtained with the ECA filtering. Its filtering performance is investigated along with the ECA-B algorithm in the following section.

### 3.3. ECA-B

The batches version of the ECA filter calculates the coefficient vector $\boldsymbol{w}_{td}$ and perform the filtering on shorter batches than the CPI. With this modification the filter has greater resistance against the non-stationer behaviour of the environment. Another great advantage is the reduced computation cost relative to the standard ECA algorithm. The filtering technique is proposed by F. Colone et al. in [6]. Let us partition the $N$ samples of the CPI to $T$ batches $t = 0 \dots T-1$. In this case one batch consist of $N/T$ samples. Let us denote the signal samples of the $t$th batch with $\boldsymbol{x}_s^{(t)}$, $\boldsymbol{x}_f^{(t)}$ and $\boldsymbol{x}_r^{t}(t)$.

$$\boldsymbol{x}_r^{(t)} = \left[x_r(tN/T) \quad x_r(tN/T+1) \quad \dots \quad x_r((t+1)N/T-1)\right]^T \tag{9}$$

(10)

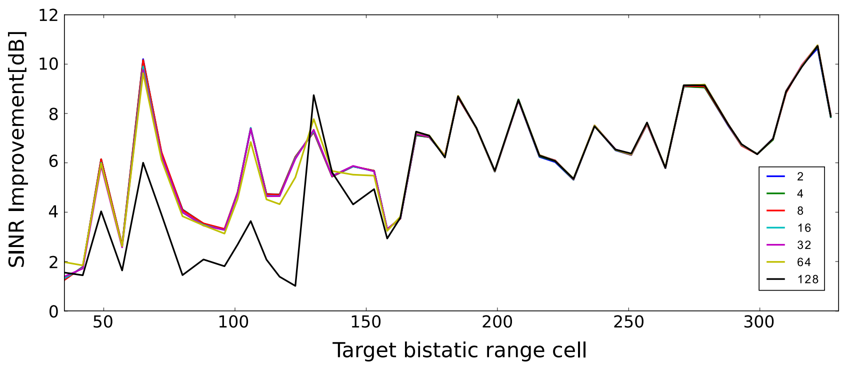


Figure 3: ECA-B algorithm improvements with different batch sizes

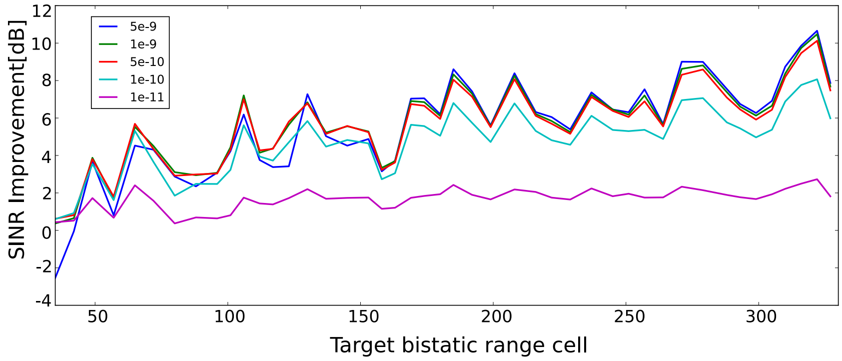


Figure 4: LMS algorithm improvements with different step sizes $\mu$

The same form holds for $\boldsymbol{x}_s^t$ and $\boldsymbol{x}_f^t$. Consequently the signal subspace spanned by the reference signal and its time and Doppler shifted replicas in the $t$th batch is denoted by $\boldsymbol{X}'^{(t)}$. Having this is mind we can calculate the filtered output signal using the following formula:

$$\boldsymbol{x}_f^{(t)} = \left(\boldsymbol{I} - \boldsymbol{X}'^{(t)} \left(\boldsymbol{X}'^{(t)H}\boldsymbol{X}'^{(t)}\right)^{-1} \boldsymbol{X}'^{(t)H}\right) \boldsymbol{x}_s^{(t)} w, \tag{11}$$

where $t = 0 \ldots T-1$. By setting the batch size shorter, the filter have the opportunity to adapt to the rapidly changing envrionment. A well known and studied disadvantage of this method is that alias echoes appears in the RD matrix along the Doppler axis beside the usefull target echo. This behaviour is investigated deeply in a theoretical way in [3]. Figure 8c illustrates the range-Doppler matrix obtained with the ECA-B filter when the whole CPI is partitioned to 32 batches. A very pleasant effect of the processing is the widening of the filter noth in the Doppler dimension. This can be clearly seen in figure 8c. The achieved improvements for different batch sizes can be seen in figure 3 with $K = 128$.

### 3.4. Least Mean Square

The LMS algorithm is an iterative implementation of the Wiener filter, where the coefficients are estimated for every new signal sample. This architecture results in a faster implementation than the SMI, ECA or the ECA-B algorithm. The LMS algorithm output at the $n$th time instant and the updated coefficient vector at the $n+1$th time instant are calculated as follows:

$$x_f(n) = e(n) = x_s(n) - \boldsymbol{w}(n)^H \boldsymbol{x}_r(n) \tag{12a}$$

$$\boldsymbol{w}_{LMS}(n+1) = \boldsymbol{w}(n) + \mu \boldsymbol{x}_{\boldsymbol{r}}(n) e(n)^* \tag{12b}$$

where $e(n)$ is the instantaneous error and $\mu$ is the step size parameter which affects the convergence rate of the filter. Step size $\mu$ must be chosen according to 13 to ensure stability and convergence.

$$0 < \mu < \frac{2}{\sum_{k=0}^{K-1} \mathbf{E}\left\{|x_s(n-k)|^2\right\}} \tag{13}$$

[2], [10] Higher step size values offers faster reactions to the changes in the environment, however the filter will suffer from misadjustment and will not able to suppress the zero Doppler interferences properly. At the same time choosing the step size too small results in sluggish filter response. In order to illustrate its effects on the filter clutter suppression performance figure 4 illustrates the achieved target SINR values for different step size parameters.

### 3.5. Normalized least mean square

The NLMS algorithm is the extension of the LMS method in a sense that the $\mu$ step size parameter is normalized with the instantaneous power of the reference signal vector. Thus the weight coefficient of the NLMS algorithm is calculated with using the following formula:

$$\boldsymbol{w}_{NLMS}(n+1) = \boldsymbol{w}(n) + \frac{\mu_n}{a + \boldsymbol{x}_r(n)^H \boldsymbol{x}_r(n)} \boldsymbol{x_r}(n) e(n)^*, \tag{14}$$

where $a$ is a small number used to prevent instability and $\mu_n$ is the modified step size parameter. In contrast to the LMS method, the step size parameter is no longer constant but it changes with the power of the reference signal and its time delayed replicas $\boldsymbol{x}_r(n-k), k = 0 \ldots K - 1$. This ensures a more stable operation and faster convergence [10]. The NLMS algorithm improvements for a variety of $\mu_n$ values can be seen in figure 5.

### 3.6. Recursive Least Squares

The RLS algorithm use a different error function than the LMS or NLMS. This method takes into consideration the earlier filter error values with reduced influence.

$$e_{RLS}(n) = \sum_{i=0}^{n} \lambda^{n-i} |e(i)|^2 \tag{15}$$

The $\lambda$ parameter is often referred to as the forgetting factor, which is chosen in the range of $0 < \lambda \leq 1$. Higher $\lambda$ values takes into account the earlier values with increased relevance. By

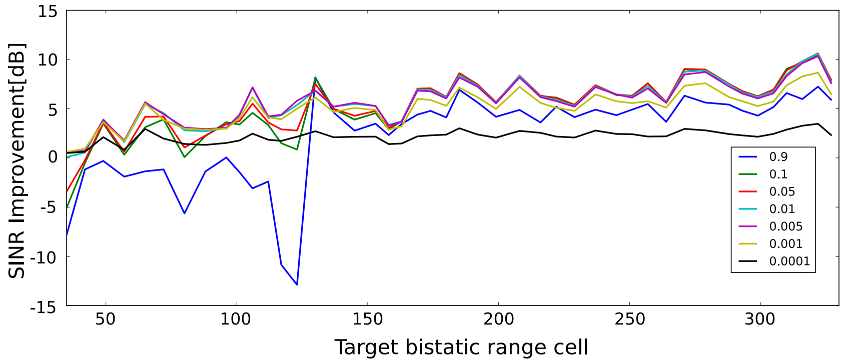


Figure 5: NLMS algorithm improvements with different step sizes ($\mu_n$)

defining the error function in the above form the filter update equations for the RLS method can be written as follows:

$$k(n) = \frac{\lambda^{-1}\boldsymbol{P}(n-1)\boldsymbol{x}_r(n)}{1+\lambda^{-1}\boldsymbol{x}_r(n)^H\boldsymbol{P}(n-1)\boldsymbol{x}_r(n)} \tag{16}$$

$$\alpha(n) = x_s(n) - \boldsymbol{W}^H(n-1)\boldsymbol{x}_r(n) \tag{17}$$

$$\boldsymbol{w}_{RLS}(n) = \boldsymbol{w}_{RLS}(n-1) + k(n)\alpha^H(n) \tag{18}$$

$$\boldsymbol{P}(n) = \lambda^{-1}\boldsymbol{P}(n-1) - \lambda^{-1}k(n)\boldsymbol{x}_r(n)^H\boldsymbol{P}(n-1) \tag{19}$$

[2], [10]. The result obtained with changing the $\lambda$ parameter can be seen in 6.

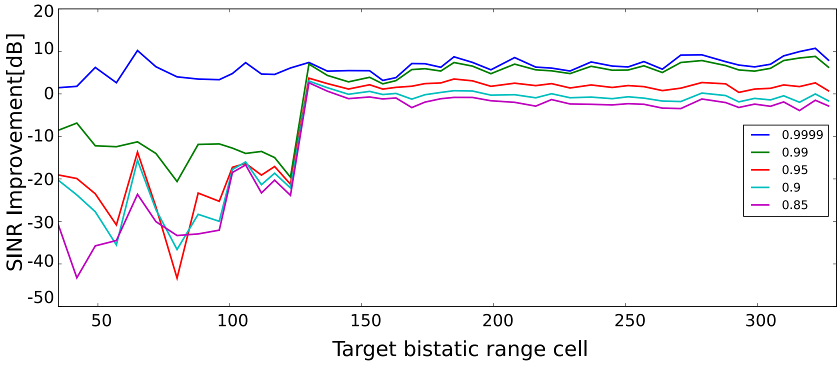


Figure 6: RLS algorithm improvements with different forgetting factors ($\lambda$).

## 4. Final results and Conclusion

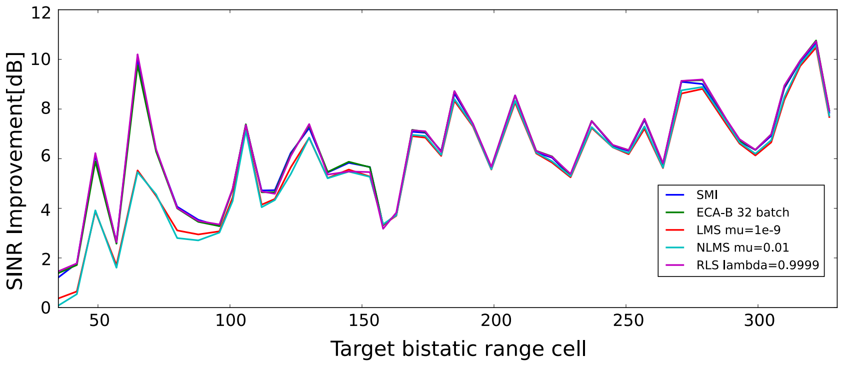


Figure 7: SINR improvements of the different time domain filtering algorithms

The final comparison of the inspected algorithms is obtained with setting the best parameters for each of the methods. Figure 7 illustrates the achieves target SINR improvements relative to the results calculated when no filtering is applied.

According to the obtained results we can conclude that the investigated iterative algorithms (LMS, NLMS, RLS) gives worst detection performance when the target in located inside the

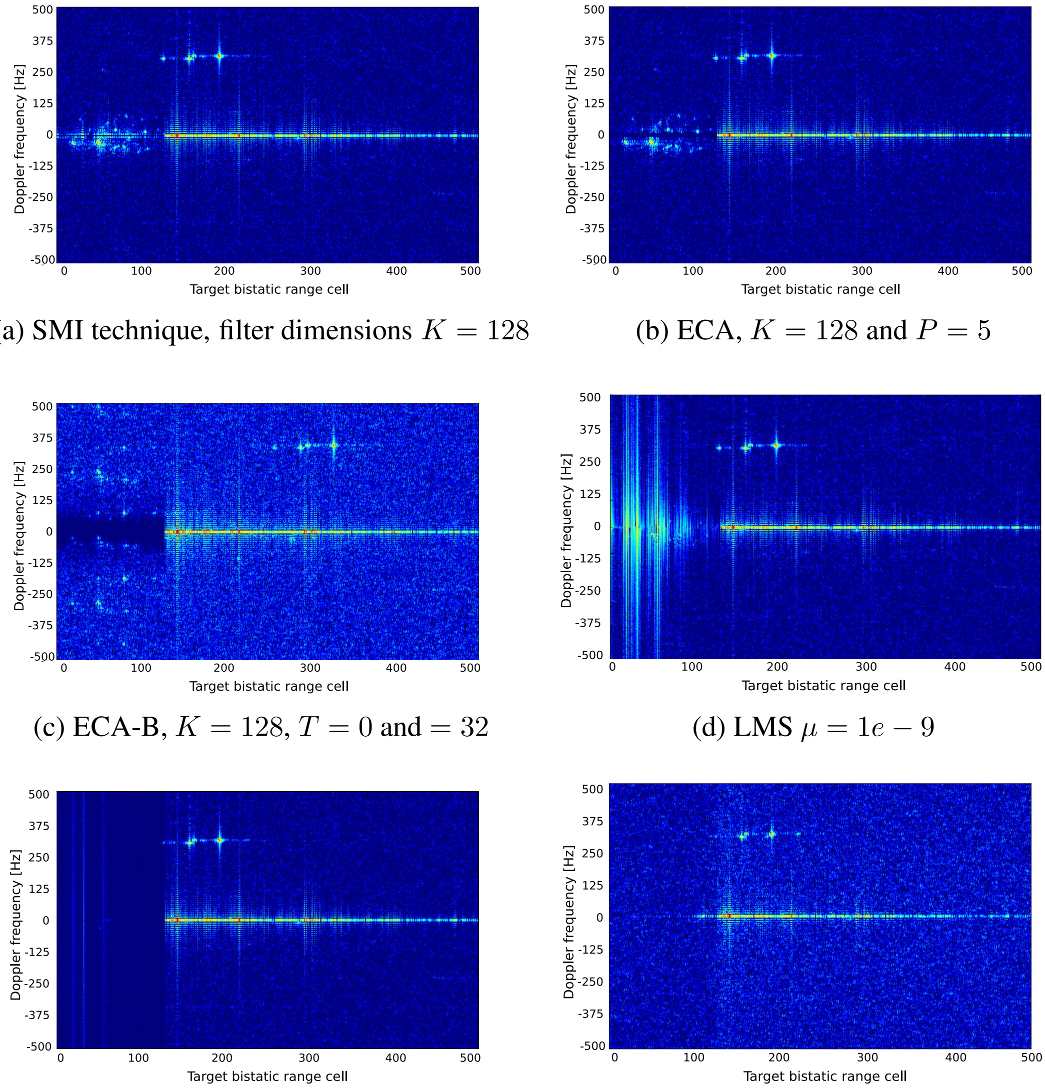


(a) SMI technique, filter dimensions $K = 128$

(b) ECA, $K = 128$ and $P = 5$

(c) ECA-B, $K = 128$, $T = 0$ and $= 32$

(d) LMS $\mu = 1e - 9$

(e) NLMS $\mu_n = 0.01$

(f) RLS, $K = 128$ and $\lambda = 0.95$

Figure 8: range - Doppler matrices with different temporal filtering techniques. The dynamic range is $50dB$.

fist $K$ range cell. Expecting the SMI method all the investigated procedures extend the filtering into Doppler domain also. This ability does improve the separation needed for targets detection, but remarkable SINR improvement is not realized. At the same time care must be taken when setting the filter parameters to not suppress the useful target reflections which is close to the zero Doppler line in the range-Doppler matrix. From among the investigated filtering procedures the ECA-B algorithm not only has good filtering performance but also reduces the computational cost compared to the ECA or the SMI method.
In this paper some fundamental temporal interference cancellation techniques have been investigated in passive radar environment. To compare their performances the realized peak-to-sidelobe level of a detected target is analyzed in the RD matrix. From among the examined

methods the batches version of the ECA algorithm seems to be a reasonable choice in systems where fast update rate and fairly wide cancellation around the zero Doppler line is a must. Following researches may focus on the effect of the reference signal purity both in the detection and cancellation.

## References


[1] Krzysztof Kulpa: 'Signal Processing in Noise Waveform Radar', (Artech House, 2013, 1st edn.), pp. 75-141

[2] Simon Haykin: 'Adaptive Filter Theory' (Prentice Hall, 3rd edn. 1995)

[3] Fabiola Colone, Claudio Palmarini, Tatiana Martelli, *et al.*:'Sliding extensive cancellation algorithm for disturbance removal in passive radar', IEEE Transactions on Aerospace and Electronic Systems, 2016, vol. 52, no. 3, pp 1309-1326

[4] Tamas Peto, Rudolf Seller:'Quad Channel Software Defined Receiver for Passive Radar Application', Archives of Electrical Engineering, 2017, vol. 66, no. 1, pp 5-16

[5] Z. Zhao, X. Wan, Q. Shao , *et al.*:'Multipath clutter rejection for digital radio mondiale-based HF passive bistatic radar with OFDM waveform', IET Radar, Sonar & Navigation, 2013, vol. 6, no. 9, pp 867-872

[6] F. Colone, D. W. O'Hagan, P. Lombardo, *et al.*:'A Multistage Processing Algorithm for Disturbance Removal and Target Detection in Passive Bistatic Radar, IEEE Transactions on Aerospace and Electronic Systems, 2009, vol. 45, no. 2, pp 1-25

[7] Tamas Peto, Rudolf Seller: 'Quad channel DVB-T based passive radar'. Int. Radar Symposium, Cracow, Poland, May 2016, pp. 1-4

[8] Christoph Schwark, Diego Cristallini: 'Advanced multipath clutter cancellation in OFDM-based passive radar systems'. IEEE Radar Conf., Philadelphia, USA, May 2016, pp. 1-4

[9] A. Di Lallo, R. Fulcoli, L. Timmoneri: 'Adaptive spatial processing applied to a prototype passive covert radar: Test with real data'. Int. Conf. Radar, Adelaide, Australia, Sept 2008, pp. 1-5

[10] Roberta Cardinali, Fabiola Colone, Chiara Ferretti, *et al*: 'Comparison of Clutter and Multipath Cancellation Techniques for Passive Radar'. IEEE Radar Conf., Waltham, USA, April 2007, pp. 1-6

[11] Fabiola Colone, Pierfrancesco Lombardo: 'Cancellation of clutter and multipath in passive radar using a sequential approach'. IEEE Radar Conf. Verona, USA, April 2006, pp.393-399